Atmos. Chem. Phys. Discuss., 10, 17263–17305, 2010
www.atmos-chem-phys-discuss.net/10/17263/2010/
doi:10.5194/acpd-10-17263-2010

Atmospheric Chemistry and Physics Discussions

Characteristics of CALIOP attenuated backscatter noise: implication for cloud/aerosol detection

D. L. Wu[1], **J. H. Chae**[1,2], **A. Lambert**[1], **and F. F. Zhang**[3]

[1]Jet Propulsion Laboratory, California Institute of Technology, Pasadena, California, USA
[2]Joint Institute for Regional Earth System Science and Engineering, University of California, Los Angeles, California, USA
[3]Harvard University, Cambridge, Massachusetts, USA

Received: 8 May 2010 – Accepted: 30 June 2010 – Published: 15 July 2010

Correspondence to: D. L. Wu (dong.l.wu@jpl.nasa.gov)

Published by Copernicus Publications on behalf of the European Geosciences Union.

Abstract

To study cloud/aerosol features in the upper troposphere and lower stratosphere (UT/LS) with the NASA's A-Train sensors, a research algorithm is developed for a re-gridded CALIOP (Cloud-Aerosol Lidar with Orthogonal Polarization) Level 1 (L1) backscatter dataset. This paper provides a detailed analysis of the measurement noise of this re-gridded dataset in order to compare the lidar measurements with other collocated measurements (e.g., CloudSat, Microwave Limb Sounder). The re-gridded dataset has a manageable data volume for multi-year analysis. It has a fixed (5 km) horizontal resolution, and the measurement error is derived empirically from the background-corrected backscatter profile on a profile-by-profile basis. The 532-nm and 1064-nm measurement noises, determined from the data at altitudes above 19 km, are analyzed and characterized in terms of the mean (μ), standard deviation (σ), and normalized probability density function (PDF). These noises show a larger variance over landmasses and bright surfaces during day, and in regions with enhanced flux of energetic particles during night, where the instrument's ability for feature detection is slightly degraded. An increasing trend in the nighttime 1064-nm σ appears to be significant, which likely causes the increasing differences in cloud occurrence frequency between the 532-nm and 1064-nm channels. Most of the CALIOP backscatter noise distributions exhibit a Gaussian-like behavior but the nighttime 532-nm perpendicular measurements show multi-Gaussian characteristics. We apply σ – based thresholds to detect cloud/aerosol features in the UT/LS from the subset L1 data. The observed morphology is similar to that from the Level 2 (L2) 05km_CLAY+05km_ALAY product, but the occurrence frequency obtained in this study is slightly lower than the L2 product due to differences in spatial averaging and detection threshold. In the case where the measurement noises of two data sets are different, the normalized PDF has proven useful for quantifying the day-night difference of the CALIOP backscatters, showing higher daytime cloud occurrence frequency in the tropical UT/LS. Other cloud/aerosol properties, such as depolarization ratio and color ratio, can be also evaluated with the

ACPD

10, 17263–17305, 2010

PDF method.

1 Introduction

Understanding the role of cirrus in a changing climate requires quantitative and reliable characterization of the vertical distribution of clouds and their variability in the upper troposphere and lower stratosphere (UT/LS) region. As an important major source of water vapor in the UT/LS, cirrus plays a critical role in climate-feedback processes through interactions with water vapor (e.g., Jensen et al., 1996; Dessler et al., 2008). However, many aspects of cirrus remain unclear, including formation and lifecycle near the tropopause (e.g., Jensen and Ackerman, 2006), microphysics (Comstock et al., 2007), and interactions with UT aerosols (Lohmann and Roeckner, 1995; Sherwood, 2002; Mishchenko, et al., 2007).

Because of the large dynamic range of ice clouds, multi-sensor observations are needed to better understand cloud properties and distributions. The CALIOP (Cloud-Aerosol Lidar with Orthogonal Polarization) instrument, launched in 2006 on NASA's CALIPSO (Cloud-Aerosol Lidar and Infrared Pathfinder Satellite Observation) satellite, has provided rich information on vertical distributions of global clouds and aerosols (Winker et al., 2003, 2007, 2009). Flying in the A-Train orbit, the nadir dual-wavelength (532 and 1064 nm) and dual-polarization (perpendicular and parallel at 532 nm) lidar has footprints collocated with CloudSat 94 GHz Cloud Profiling Radar (CPR) (Stephens et al., 2002) and a suite of passive imagers/sounders. The CALIOP and CloudSat measurements are aligned with Aura MLS (Microwave Limb Sounder) measurement tracks within 10 km in cross-track distance since May 2008, which extended collocated cloud measurements to high-frequency microwaves. Together with the infrared (IR) and visible imagers/sounders in the A-Train, the collection of nearly-coincident-and-collocated observations opens an unprecedented opportunity for cloud research.

Like other remote sensing techniques, the performance of CALIOP cloud/aerosol detection depends on measurement noise and size of measurement volume. The detec-

ACPD
10, 17263–17305, 2010

tion threshold to derive occurrence frequency of cloud/aerosol features is particularly sensitive to these variables (Wu et al., 2009). Separating between clear and cloudy skies in noisy measurements is not trivial, and comes down to a fundamental question – what is a cloud? For fair cloud/aerosol detection, one would want a sensor that has a stable noise level such that a constant threshold can be applied globally to all the measurements. Compared to CALIOP backscatters, CloudSat reflectivity noise is relatively stable from day to night and from orbit to orbit (Tanelli et al., 2008). CALIOP noise can vary by more than two orders of magnitude within an orbit, which makes the cloud/aerosol detection threshold a strong function of space and time. This noise map or distribution will ultimately affect patterns of the features detected. Detailed descriptions on the CALIOP instrument calibration and performance can be found in Hunt et al. (2009), whereas false detection and misclassification in the cloud/aerosol feature detection are discussed in Liu et al. (2006) and Vaughan et al. (2009).

The CALIPSO Level 2 (L2) 5-km cloud and aerosol layer products (i.e., 05km_CLay and 05km_ALay) are based on the algorithm described in Vaughan et al. (2009), which employs a detection scheme with variable horizontal lengths on the attenuated total 532-nm backscatter. In order to detect weak features such as thin cirrus, polar stratospheric clouds (PSCs), and aerosol layers, the L2 algorithm uses an adaptive multi-profile averaging scheme to search for coherent features from consecutive profiles within 5, 20, and 80 km in distance depending on feature strength and spatial correlation. The L2 algorithm widens a search, if necessary, to 80 km along track in order to enhance its ability to detect PSCs and aerosol layers. In addition, cloud/aerosol layers must meet a requirement for minimum thickness. As a result, the features detected by the L2 algorithm represent the statistics at a mixed spatial resolution (i.e., mixed measurement volume).

To initiate a multi-sensor cloud study with the A-Train instruments (in particular, with MLS multi-frequency radiometry), in this paper we develop a research algorithm for cloud/feature detection from a re-gridded CALIOP level 1 backscatter dataset. Here we seek a better understanding of the statistics of CALIOP measurement noise and

ACPD
10, 17263–17305, 2010

cloud/aerosol features with this research algorithm by applying it to the multi-year dataset. For fair cloud/aerosol detection it is imperative to keep the feature detection criteria fixed since the statistics of these features may change with space and time in terms of size and inhomogeneity. More importantly, a subtle change in the detection method may affect the trend or variation derived for cloud/aerosol statistical properties. Thus, the detection method should be independent of the feature variability as much as possible. However, CALIOP has larger variability in measurement noise, which makes this goal more difficult to achieve, compared to other A-Train sensors. We will quantify these noise characteristics to determine statistical significant variations of CALIOP cloud/aerosol features (e.g., seasonal, international and diurnal variations).

In addition to the basic noise properties, such as mean (μ) and standard deviation (σ), of the attenuated total (TOT) and perpendicular-polarization (PER) backscatters and their spatial and temporal variations, we adopt the normalized probability density function (PDF) to characterize the measurement noise and weak cloud/aerosol features. Our analyses are focused on the cloud/aerosol detection in the UT/LS region where the results are sensitive to the lidar noise, instrument calibration and sensitivity (Hunt et al., 2009). We choose to derive the measurement noise properties empirically from the re-gridded dataset because the results will include both expected and unexpected contributions after the instrument calibration. Since the re-gridded dataset will be used for further A-Train multi-sensor studies, the derived properties for CALIOP measurement noise and cloud/aerosol features will serve as the basis of inter-comparisons with other sensors. As an example, we will discuss cloud/aerosol statistical properties when two datasets have very different noise properties (e.g., daytime and nighttime), and implications of these derived CALIOP cloud statistics for other scientific investigations.

ACPD
10, 17263–17305, 2010

2 Data and methods

The provisional release (version 2.0) of Level 1 (L1) data are used in this study, which contain CALIOP attenuated backscatter coefficients in $km^{-1}\,sr^{-1}$, $\beta'(z)$, and auxiliary data such as molecular and ozone density profiles provided by NASA's GMAO (Global Modeling and Assimilation Office). Data in the original L1 file have 583 vertical levels with resolutions from 30 m near the surface to 300 m in the stratosphere, and horizontal resolution of 300 m (Winker et al., 2009). For the long-term statistical analyses in this study, we reduce the data resolution and therefore the data volume by aggregating them vertically and horizontally. The new dataset have 194 vertical levels with a 3 times coarser resolution than the original L1 file, and a horizontal resolution of 5 km. The vertical resolutions of the re-gridded dataset become 90 m at −0.5–8.2 km, 180 m at 8.2–20.2 km, 540 m at 20.2–30.1 km, and 900 m above 30.1 km. The 5 km bin size will render a uniform horizontal resolution for all altitudes below 40 km in the re-gridded data. The non-uniform vertical resolution is taken into account by weighting error statistics based on the measurement integration time as done in other studies (e.g., Liu et al., 2006).

Figure 1 shows two examples of the attenuated backscatter profiles from the CALIOP data. The daytime measurements, much noisier than nighttime data, only reveal some hints of the molecular scattering background in the bottom of the 532-nm TOT profile. However, this atmospheric background is clearly seen in the nighttime 532-nm TOT data. Measurement noise and molecular scattering are smaller in the 532-nm PER data, but the cloud/aerosol signals in the 532-nm PER backscatters are also weaker. The daytime 1064-nm and 532-nm TOT noise is similar, but in nighttime the 1064-nm data are noisier than 532-nm.

For each backscatter profile we first estimate its clear-sky atmospheric background due to the molecular scattering. This background, denoted by $\beta_0(z)$, is attenuated by the two-way molecular and ozone transmission T^2_{mol} and T^2_{o3}, namely, $\beta_0(z)T^2_{mol}T^2_{o3}$. We use the air number density profiles in the L1 file and the analytical relations, as de-

ACPD
10, 17263–17305, 2010

scribed in the CALIPSO algorithm theoretical basis document (Hostetler et al., 2006), to obtain the model-estimated atmospheric background.

The modeled molecular profile should represent the clear-sky atmospheric backscatter profile well if the instrument is accurately calibrated. In reality, the instrument calibration may be not perfect and have systematic errors. On the other hand, the atmospheric background model may exclude other backscatter contributions (e.g., stratospheric aerosols) and their attenuation/scattering effects, which can come from ejection of biomass burning and volcanic eruption (e.g., Fromm et al., 2008; Thomason and Pitts, 2008). To investigate potential error in the modeled molecular scattering, we fit it to the clear-sky data in form of $\alpha \cdot \beta_0(z) T_{\mathrm{mol}}^2 T_{\mathrm{o3}}^2$, where α is a scaling factor to give the best match to the data. For the perfect model, instrument calibration, and clear sky, α should be equal to unity. In this fitting, the key step is to obtain the clear-sky atmospheric measurements within each profile, and we employ the iterative approach used for CloudSat data (Tanelli et al., 2008; Wu et al., 2009), except that in the CALIOP case the clear-sky atmospheric background is a function of height. To define the "clear-sky" measurements in a rough way, we exclude the entire profile if any backscatter value exceeds $0.004\,\mathrm{km}^{-1}\,\mathrm{sr}^{-1}$ in 532-nm TOT. Note that this empirical screening approach for clear skies will likely contain contributions from stratospheric clouds/aerosols. In addition, the measurement error can cause a noisy fit. Thus, in monitoring α properties, we average daily values, but separately for day and night, to examine small systematic variations in α.

The procedure for fitting the "clear-sky" profiles is as follows. We start with the modeled molecular profile $\beta_0(z) T_{\mathrm{mol}}^2 T_{\mathrm{o3}}^2$ and subtract this profile from the observed backscatter profile $\beta'(z)$. The difference, i.e., $\Delta\beta(z) = \beta'(z) - \beta_0(z) T_{\mathrm{mol}}^2 T_{\mathrm{o3}}^2$, may contain cloud/aerosol features (positive values) and strongly-attenuated backscatter (negative values). In the first step of screening, we reject very large outliers with $\Delta\beta(z) > 10^{-3}\,\mathrm{km}^{-1}\,\mathrm{sr}^{-1}$, and estimate the mean and standard deviation (μ and σ) of $\Delta\beta(z)$ from the remaining backscatters within the profile at altitudes greater than 400 m above the surface. Note that scaling factor α and μ are related through

ACPD
10, 17263–17305, 2010

$\mu \equiv < \Delta\beta > = (\alpha - 1) < \beta_0(z) T_{mol}^2 T_{o3}^2 >$. For the subsequent iterations, we replace $\Delta\beta(z)$ with $\beta'(z) - \alpha\beta_0(z) T_{mol}^2 T_{o3}^2$ and screen the $\Delta\beta(z)$ profile again using the calculated μ and σ by rejecting the measurements that are $>3\sigma$ from the mean on both sides. The σ value is scaled for each height bin according to integration time. The μ and σ are re-calculated from the screened data, which leads to a new scaling factor α. We repeat these steps until convergence (i.e., negligible change) is reached for μ, σ and α or the number of iteration reaches 10. Convergence is usually achieved within 3–4 iterations, and non-convergent cases are discarded. The final μ, σ and α are output as the measurement error for this profile. If the number of remaining data points in the last iteration is less than 100, the fit is considered not reliable and these outputs are assigned to a bad data value of −999. We have applied the same screening estimation procedure for CALIOP 532-nm TOT and PER backscatters, and for the 1064-nm backscatter profiles.

Figure 2 shows an orbit of the estimated σ values from daytime and nighttime backscatters of this re-gridded data. The μ value of $\Delta\beta(z)$ error is usually smaller than σ, and cloud/aerosol detection is mostly determined by σ. As shown in Fig. 2, the nighttime 532-nm PER backscatter σ values are exceptionally lower than other cases, which could yield a higher signal-to-noise ratio for weak cloud/aerosol signals if these features produce a significant depolarization ratio. However, this low backscatter σ makes additional noise sources stand out, which would not be able to be seen otherwise. These added measurement noises and their characteristics must be carefully dealt with before implementing cloud/aerosol detection schemes. For examples, in Fig. 2 the measurement noise increases due to high dark counts (Hunt et al., 2009), as seen in the nighttime 532-nm PER σ in the radiation-hard regions such as the South Atlantic Anomaly (SAA) and auroral ovals. The added noise induced can be 5–10 times greater than the normal nighttime σ values. Unlike the 532-nm measurements, the 1064-nm backscatters do not exhibit obvious dependence on the SAA because the 532 nm detetectors are photomultiplier tubes (PMTs) and more susceptible to radiation effects than the 1064 nm avalanche photodiodes (APDs) (Hunt et al., 2009). As discussed in Hunt et al. (2009), PMTs have modest quantum efficiencies with rela-

ACPD
10, 17263–17305, 2010

tively low dark noise that should obey the Poisson statistics; whereas APDs have high quantum efficiencies but with high Gaussian-like dark noise.

High-degree transiency is also evident in the CALIOP backscatter σ at a profile-to-profile scale (Fig. 2). This large σ variation affects the cloud/aerosol detection throughout a backscatter profile. The cause of the profile-to-profile σ variability is likely associated with spatial variations of cloud/aerosol/surface albedo. Because of the transiency and heterogeneity in σ, detecting cloud/aerosol features using information from adjacent profiles should be done with caution. If noise level is substantially non-stationary, imposing a uniform threshold to multiple profiles (for example, over 80 km) would increase the false-positive error in the features detected for a wider domain. By the same token, the rapid transition of measurement noise from daytime to nighttime, as shown in the 532-nm PER backscatters, appears to be challenging for developing a good cloud/aerosol detection algorithm.

The estimated error characteristics are sensitive to systematic residuals left from the instrument calibration or model error (e.g., stratospheric aerosols). Figure 3 shows that the daily averaged scaling factor α is seen near unity for the 532-nm nighttime data, but can vary between 5% and 10% during daytime. Within a given day, the α value can have much larger variability due to measurement noise in a single profile. The nighttime 532-nm α value exhibits a variation of <2% over the two year period. Even though the nighttime 532-nm data are best calibrated, a drop of ~2% in α between version 2.01 and 2.02 (switching the GMAO data from v5.10 to v5.20) is evident. A much larger (~10%) drop in α is in the daytime 532-nm data on 6 October 2008, but it is not associated with the version change. It is unclear what caused such a large systematic drop in the daytime 532-nm data. In addition, the daytime 532-nm α value shows a significant seasonal variation, which is much larger than the nighttime α. Because of the higher noise, the daytime fits could include some weak cloud/aerosol features (above the atmospheric molecular background) and attenuated values (below the background) in the screened "clear-sky atmospheric molecular background". We tested this noise threshold effect with the nighttime 532-nm data by increasing the outlier-rejection

ACPD
10, 17263–17305, 2010

threshold from 3σ to 80σ, and found the nighttime α value would contain a significant seasonal variation as well. The 1064-nm backscatter generally has a higher α value (1.1–1.6 for daytime and 0.9–1.4 for nighttime) than the 532-nm channel and exhibits a large seasonal variation in both daytime and nighttime data, which is different from the daytime 532-nm result. As aforementioned, the seasonal variations may be caused by the poorly screened "clear-sky atmospheric background" associated with this approach for noisy data, and the contaminated α would be slightly higher at 1064 nm than 532 nm since the backscatter ratio of the stratospheric aerosols is larger at the 1064 nm channel. However, the atmospheric contamination should be same for both day and night, and the inconsistent seasonal variations in day-night α values and the increasing trend in the nighttime values imply some issues remaining in the calibrated 1064-nm backscatters. As also seen in Fig. 3, the daily averaged α values exhibit large seasonal variations with lower values in December and January, as well as large day-night differences. Nevertheless, the day-night differences are greatly reduced in version v2.02.

In the analysis hereafter, we ignore the seasonal variations in α and use α=1.0 to remove the background molecular backscatter for all the CALIOP channels except the 532-nm perpendicular. The μ and σ of measurement noise are estimated using the aforementioned iterative-screening method but only from $\Delta\beta(z)$ at $z > 19$ km.

3 Morphology of CALIOP backscatter noise

To characterize the CALIOP backscatter noise, we map the monthly-mean μ and σ estimated from the measurements above 19 km, separately for daytime and nighttime. January 2008 is chosen to illustrate the noise properties but other months reveal similar characteristics. As described in Liu et al. (2006) and Hunt et al. (2009), PMTs used by the 532-nm channels have modest quantum efficiencies with relatively low dark noise that should obey the Poisson statistics; whereas APDs by the 1064-nm channel have high quantum efficiencies but with high Gaussian-like dark noise. For a num-

ACPD
10, 17263–17305, 2010

ber of photons >5, the Poisson distribution can be approximated well with a Gaussian distribution, which is convenient for comparing noise and determining detection thresholds. In addition to the detector noise and other calibration errors, CALIOP backscatter measurements contain noise induced naturally by the atmosphere and surface. The primary difference between daytime and nighttime CALIOP backscatter noise is dominated by the background scattering sunlight, which is additive, Gaussian in nature and highly variable depending on surface/atmospheric albedo. As a result, the CALIOP sensitivity to clouds/aerosols and the variability of features detected will depend on the distribution and variation of these noise sources, especially for weak features in the upper troposphere and lower stratosphere.

The daytime μ (Fig. 4) is nearly zero everywhere, except in the SAA region where it is slightly negative. However, the σ value varies highly with surface type and cloud albedo. Cloud and surface albedo effects appear to modulate the 532-nm σ by a factor of 2-5 with higher values usually in cloudy/snowy/icy regions (which are evident in CALIOP quick-look browse images) or over landmasses (e.g., desert). Compared to the 532-nm measurements, the 1064-nm σ map shows more distinct contrast between land and ocean mostly in the Southern Hemisphere.

The nighttime CALIOP noise (Fig. 5), although generally lower than the daytime in terms of the μ and σ values, reveals features related to detector error in response to the South Atlantic Anomaly (SAA) and other high-latitude geomagnetic activities. These geomagnetic features are more pronounced in the 532-nm than in the 1064-nm measurements. The 532-nm PER and TOT are respectively ~50× and ~5× less noisy than the measurements in the geomagnetic-active regions. In the SAA region, the enhanced radiation can induce current spikes in the PMT detectors and lead to higher dark count noise. The radiation-induced dark counts in PMT become only important during nighttime when the solar background noise is absent.

More complete statistical properties of the CALIOP noises are presented in Figs. 6–8 in terms of the normalized probability density function (PDF). The PDF is derived from the attenuated backscatters with the molecular background subtracted (see Fig. 1).

ACPD
10, 17263–17305, 2010

The number of samples in each backscatter value bin is divided first by the total number for normalization and then by the bin sizes to yield probability density. Since cloud/aerosol scatterings produce positive backscatters, the PDF of negative values, generally speaking, reflects characteristics of measurement noise, which can be Gaussian or non-Gaussian depending on noise sources. However, clouds/aerosols also attenuate the molecular background scattering below them, which could skew the distribution of the background-removed backscatters at lower altitudes.

In Figs. 6–8 the rising PDF at small backscatter values is indicative of the measurement noise, which includes all error sources such as detector noise, calibration error, and the solar background. For the noise with a zero mean both positive and negative values should yield a consistent PDF in the noise part of the distribution. In the case where measurements are dominated purely by noise, usually at altitudes >19 km, the positive and negative PDF domains should overlap each other, which is evident in Figs. 6–8 at 21.7 km. In the presence of clouds/aerosols, the positive PDF domain will exhibit an extended distribution above the negative PDF domain. In reality measurement noise may not be purely Gaussian or multi-Gaussian. Non-Gaussian cases require special care in cloud/aerosol detection since the detection threshold needs to be sufficiently high to account for the false-positive rate from the non-Gaussian distribution.

Figure 6 shows the PDFs of the 532-nm PER measurements. The daytime PDFs of positive- and negative values overlap at small ($<3\sigma$) backscatter values. This consistency is particularly striking at 21.7 km where no significant cloud/aerosol features are present and both PDFs resemble a Gaussian noise distribution. For the measurements at lower altitudes, the PDFs of positive backscatter have an extended distribution, representing contributions from clouds or aerosols, whereas the PDF of negative backscatter remains roughly as expected. For cloud/aerosol feature detection with the daytime 532-nm PER data, a threshold of $>3\sigma$ is needed to minimize the false detection rate. The nighttime 532-nm PER noise (lower panels in Fig. 5) exhibits complex noise characteristics as the measurement noise reaches a very low level. Non-Gaussian or

ACPD
10, 17263–17305, 2010

multi-Gaussian noise characteristics start to appear at backscatter <10σ. Because of the complex nature of low-level nighttime noise, in order for robust cloud/aerosol detection with the nighttime 532-nm PER data, a higher (>10σ) threshold is usually needed to avoid a significant number of false detections.

Figure 7 shows the PDFs of the 532-nm TOT measurements in the tropics. For the daytime the noise PDFs of negative and positive values agree well with each other. The nighttime PDFs of the 532-nm TOT are less complicated than those in the 532-nm PER cases, resembling single-Gaussian noise characteristics in most cases. However, it requires more in-depth investigations to understand and quantify how much is due to instrument/calibration errors and how much is from the unmodeled signals such as stratospheric aerosols. Although stratospheric aerosols are difficult to detect, their contributions can be inferred from differences between the PDFs of positive- and negative-value backscatters at night. For example, at 21.7 km the positive-value PDF exhibits a higher probability than the negative-value PDF, indicating either a bias in the estimated background backscatter or potential contributions from stratospheric aerosols.

Similar to the result in Fig. 6 for 532-nm PER, the cloud PDF of the nighttime 532-nm TOT at 16.4 km shows a drastic change in slope at the backscatter value of $\sim 10^{-2.5}\,\mathrm{km}^{-1}\,\mathrm{sr}^{-1}$, which is buried underneath the noise in the daytime measurements. At lower altitudes the negative-value PDF can rise above the positive-value one because there exist a significant number of attenuated backscatter cases. In these situations, the backscatters beneath cloud/aerosol layers are severely attenuated such that these values can fall below the estimated molecular scattering background, resulting in negative $\Delta\beta(z)$ values. This attenuation effect is more evident in the nighttime PDFs than in the daytime mostly because of smaller measurement noise in the night. These attenuated cases are also referred to as "obscured" regions elsewhere in this paper. They could have an impact on the scaling factor α derived in Fig. 3 because there are always some unscreened values within the 3σ threshold. These unscreened values from the strong attenuation would weight the fit to produce a smaller α, which might explain the seasonal variation of the daytime α seen in Fig. 3 for the 532-nm

ACPD
10, 17263–17305, 2010

channel.

Compared to the 532-nm TOT, the 1064-nm TOT data bear many similarities in PDF characteristics but with a slightly higher σ (Fig. 8). Unlike the 532-nm, the nighttime 1064-nm data do not have the sharply higher negative-value PDFs at lower altitudes because the molecular scattering background and attenuation due to cloud/aerosol scattering are ~16× weaker at 1064 nm. Moreover, the large 1064-nm measurement noise makes it almost undetectable for the attenuation effect on the molecular background.

4 Implications and challenges for feature detection

Large variabilities of CALIOP measurement noise, especially the noise variation and distribution pattern, have direct impacts on cloud/aerosol detection. CALIOP backscatters should be at least 3-σ above the estimated noise background in order to be significant as cloud/aerosol features. The false-positive rate under this rule is ~0.3% if the noise is purely Gaussian. If cloud occurrence frequency is small (say, 1%), the 0.3% false rate can contribute a significant percentage as cloud occurrence since a 0.3% of 99% clear-sky measurements would provide an additional ~0.3% cloud occurrence, which is a relative 30% error for clouds. This error would drop to ~10% if the detection scheme requires at least two consecutive vertical layers to be 3σ significant. In non-Gaussian cases the false-positive rate is likely even higher, and tighter requirements are often needed for feature detection. As shown in Fig. 6, the nighttime measurement noise is usually non-Gaussian or multi-Gaussian.

To ensure reliable feature detection, we tested a range of detection thresholds using the estimated σ value for each profile, and settled on the thresholds listed in Table 1. The selected thresholds allow us to aggressively exclude the clear-sky background with a very low false-positive rate, including the non-Gaussian part of the noise. In other words, some background aerosols (in the stratosphere and troposphere) will fall under the thresholds; and some PSC features will be missed as well. In the twilight zones,

ACPD
10, 17263–17305, 2010

both daytime and nighttime σ rules will produce either underestimated or overestimated cloud/aerosol statistics because the σ value can vary rapidly (Fig. 2). To prevent the threshold from reaching too high or too low, we amended the σ-based detection rules with a maximum/minimum bound.

In addition to the σ rule from Table 1, we also require that a feature must appear in two or more consecutive vertical bins. This additional requirement further reduces the false-positive error as described above, and this strict rule is needed for the cloud detection near the tropopause where cloud occurrence frequency drops sharply with height. Because the σ used for cloud/aerosol detection is estimated on a profile-by-profile basis, the region with a higher σ, such as the SAA and landmasses, will inevitably have poorer detecting ability, leading to potential sampling artifacts in the observed cloud/aerosol pattern. The σ-based detection has less impact on the observed backscatter pattern than on the cloud/aerosol occurrence frequency since the intensity average is still accurate as long as there is no significant bias in the data. Figure 9 show some examples of the features detected from the nighttime orbit in Fig. 2. As seen in the features detected and missed, the thresholds in Table 1 are relatively conservative by rejecting some of the tenure aerosol and cirrus features. Since these thresholds depend on the measurement volume and atmospheric features of interest, different values will likely be used if the backscatters are averaged to match other instrument measurements (e.g., MLS).

Figures 10–11 show zonal mean statistics of the cloud/aerosol features observed from the σ detection criteria described above. The mean backscatter is computed from the background-corrected values, i.e., $\Delta\beta(z)$, and averaged into a given latitude and altitude bin. Consistent with the cloud/aerosol occurrence frequency, only $\Delta\beta(z)$ detected as a feature are included in the average. Although morphologies of the mean backscatter and cloud/aerosol occurrence frequency are generally consistent, differences are evident in the zonal distributions. For example, in the tropical upper troposphere, the mean 532-nm and 1064-nm TOT backscatter in January 2008 have a clearly higher value just south of the equator, which is not revealed in the occurrence

ACPD
10, 17263–17305, 2010

frequency. Also in the 532-nm PER case, the high percentage occurrence frequency at northern high latitudes does not yield a higher backscatter at the same latitudes. The attenuated backscatter measurements are more closely related to volume extinction or water content of cloud/aerosol layers, which is a desirable quantity to compare with cloud observations from different sensors.

Compared to the statistics from CALIPSO Level 2 (L2) 05km_CLay and 05km_ALay products (Fig. 10g and Fig. 11g), the percentage of features detected in this study (Fig. 10e and Fig. 11e) is generally lower. Derived from the 532-nm TOT measurements, these L2 products employ a detection scheme with variable horizontal lengths, which explains most of the differences seen here. This adaptive horizontal averaging scheme for feature detection allows the L2 algorithm to detect more features with weak backscatter but large spatial extent, such as thin cirrus, polar stratospheric clouds (PSCs), and aerosol layers (Fig. 10g and Fig. 11g). By searching coherent features from consecutive profiles within 5, 20, and 80 km in distance (Vaughan et al., 2009), the L2 algorithm may widen the search domain, if needed, to 80 km along track in order to enhance its ability to detect PSCs and/or aerosol layers. This approach will increase the percentage of feature cover if they are associated with a large spatial extent. As a result, the L2 algorithm can detect more stratospheric features than the fixed 5-km algorithm developed in this study, largely because of the spatial resolution differences.

However, the features detected with mixed spatial resolutions would complicate interpretation about the observed cloud/aerosol statistics since these statistics depend on spatial inhomogeneity as well as occurrence frequency of these features, both of which are unknown and highly variable in reality. In this study we choose a detection method with the fixed 5-km spatial resolution and apply the σ detection rule to each profile independently. As expected, therefore, the algorithm in this study detects fewer PSC (limited by the large noise) than the L2 products. As shown later in this section, knowledge of measurement noise variations is important for interpreting changes (e.g., trends) of the features detected with any σ-based algorithms. Moreover, the research algorithm can be applied to the CALIOP data averaged at a fixed resolution wider than

ACPD
10, 17263–17305, 2010

5 km. In those cases (not shown here), the measurement noise is lower and more features with a coherent spatial distribution can be detected. As the measurement noise is reduced by averaging, its characteristic needs to be re-evaluated because other error sources may become more important.

The cloud/aerosol features detected in this study, as well as in the L2 data, show strong seasonal variations. How much of these variations is real and how much is due to variations in the measurement noise? Since the CALIOP observations in the upper troposphere have an unprecedented vertical resolution, validating these global seasonal variations to the accuracy of interest appears to be difficult. On one hand, CloudSat does not have the same sensitivity to the cirrus clouds as CALIOP. On the other hand, observations from passive limb sounding, typically with a 1–3 km vertical resolution and long horizontal averaging, cannot be compared directly with the results acquired at CALIOP resolution. Nonetheless, a self-consistent validation can be carried out to partially address the aforementioned question. Figures 12–14 are created to address this issue using the monthly statistics in the tropical upper troposphere.

Figure 12 shows the cloud/aerosol features obtained by this study and the L2 algorithm at 15 km. The daytime 532-nm and 1064-nm TOT measurements have similar amplitudes, both greater than the 532-nm PER values. The 532-nm depolarization, δ, is approximately 0.3 for the daytime and ~0.45 for the nighttime despite the strong seasonal variations in cloud fraction. Sassen and Zhu (2009) reported a slightly larger (~0.41) daytime δ at 15 km in the tropics, and a smaller (~0.28) nighttime δ, using the attenuated backscatters not corrected by the molecular background They also reported an enhanced nighttime δ in the SAA region. The difference between the nighttime δ values reported in these studies and the enhancement over the SAA suggest that the depolarization ratio is sensitive to the measurement noise and the thresholds used for feature detection (Table 1). Also shown in Fig. 12, the cloud/aerosol occurrence frequency depends strongly on the threshold used, which is reflected in both daytime and nighttime observations. Although the mean backscatter values are similar, the day-night differences are nearly a factor of 2 in occurrence frequency. The L2 daytime

ACPD
10, 17263–17305, 2010

cloud/aerosol frequency shows a systematically higher percentage than the 532-nm TOT result obtained in this study. Although no significant trend is found in both daytime and nighttime depolarization ratios, there is a decreasing trend in the 1064/532 color ratio. Given that the version 2 1064-nm backscatters are still preliminary, we will revisit the color ratio trend with the newer versions of the data.

There is a subtle trend in the noise of the 1064-nm channel, which may explain the increasing differences of cloud/aerosol frequency at 15 km between the 532-nm and 1064-nm measurements (Fig. 12). Figure 13 shows the time series of the mean single-profile σ of CALIOP backscatters in 2006–2008, which is estimated separately for daytime and nighttime. Although the daytime noises are closer to each other ($\sigma_{1064\_TOT} > \sigma_{532\_TOT} > \sigma_{532\_PER}$) with similar seasonal variations, the nighttime σ values differ by more than an order of magnitude. There exist some seasonal variations in the daytime σ. For example, the noise in February 2007 is higher than in May 2007, which means that for the same occurrence frequency the σ-based algorithm would detect fewer features in Feburary 2007. In other words, the ratio of February-to-May feature occurrence frequency in 2007 is likely to be slightly higher than what is shown in Fig. 12, which should be similar to the ratio for the averaged backscatter in Fig. 12, as suggested by the nighttime observations. On the other hand, the nighttime σ_{532_PER} and σ_{532_TOT} are roughly constant over the period of two years, which indeed produces a similar February-to-May ratio between feature occurrence frequency and the averaged backscatter. The σ_{1064_TOT}, however, exhibits a significant increasing trend, which is consistent with the dark count increases in the 1064-nm channel (Hunt et al., 2009). The increasing σ_{1064_TOT} implies a reduced ability in feature detection with this channel. The increasing difference between the 532- and 1064-nm feature occurrence frequencies at 15 km (Fig. 12) is a manifestation of this degraded sensitivity in the 1064-nm channel.

At the heights near and above the tropopause, where feature occurrence drops sharply with height, the feature detection from various methods begins to show some significant differences. As seen in Fig. 14, this study produces a smaller daytime

ACPD
10, 17263–17305, 2010

occurrence frequency at 18 km than the L2 data, and little seasonal variations are found at 18.5 and 19 km where the L2 data show larger frequencies with a decreasing trend. It warrants further investigation whether the decreasing trend is related to the stratospheric aerosol trend reported by Vernier et al. (2010). At these altitudes, cloud/aerosol-induced backscatters are marginally detectable, especially during daytime when the measurement noise is high, and the observed seasonality is associated with large uncertainty. The monthly-averaged backscatters from clouds/aerosols at 18 km are 1–2% of the values at 15 km (Fig. 12), and the day-night differences in monthly backscatters and occurrence frequencies reflect both the noisy nature of the measurements, and the different detection thresholds used for the daytime and nighttime data. Since the nighttime backscatters generally have lower noise, the seasonality observed from the nighttime data at 18 km is believed to be more reliable. Nonetheless, the nighttime occurrence frequencies from the two algorithms are generally consistent except for December 2006 and March 2008. In this study we find that the seasonal variations of the nighttime backscatter and the occurrence frequency are very similar at these altitudes. Analyzing the CALIOP data from June 2006 to February 2007, Fu et al. (2007) found no clouds above 19 km and observed a ~0.05% occurrence frequency at 18.5 km and 0.5% at 18 km. This study shows that the 0.1 % per km level is close to the noise floor or the stratospheric background, and the TTL (tropical tropopause layer) top has a strong seasonal variation, as expected for deep convective climatology. In the case where the desired signals are close to the noise floor, the convolution of signal and noise statistics would make comparisons of different data sets more challenging. Hence, a more careful and detailed analysis on the measurement noise statistics is needed.

Wu et al. (2009) suggested to compare statistics of two datasets in terms of the normalized PDF even if these measurements have significantly different noise properties. The method used requires that two data sets have the same measurement volume. If the measurements are associated with different volumes, one needs to average one with the higher spatial resolution to match that of the lower. The normal-

ACPD
10, 17263–17305, 2010

ized PDF method avoids use of artificially-imposed thresholds and can be applied to observations acquired by different sensors on different platforms. As long as these data sets are sufficiently sampled, they represent the statistical ensemble and the PDF comparisons will yield useful characterization on measurement noise, bias, sensitivity limitation, and cloud/aerosol statistics of the ensemble. For example, monthly CALIOP data would provide enough samples to characterize day-night differences. Because clouds are short-scale stochastic processes, it is reasonable to assume that they are independent and repeatable at the same geographical region even though they are not measured simultaneously.

Here we apply the PDF method to the CALIOP backscatter measurements for daytime and nighttime cloud/aerosol features. Because the CALIOP noise differs substantially between day and night, Fig. 15 is made to compare the daytime and nighttime PDFs of background-removed backscatter measurements without any detection thresholds imposed. As shown in Fig. 15, the daytime and nighttime measurements in January 2008 exhibit the measurement noises (i.e., the rising portion of the normalized PDF at small backscatter values) arose from different sources. At altitudes >15 km, the noise PDF (especially during daytime) becomes so important that it convolves with the cloud/aerosol PDF and makes the two hardly distinguishable. As a result, the PDF with a larger noise, such as the daytime PDF, would rise sooner at larger values to appear having a higher probability. This situation occurs where the backscatter values are less than the daytime noise but greater than the nighttime noise. The portion of the PDF dominated by noise does not reflect the real cloud/aerosol PDF difference, and therefore is excluded in the PDF difference curve.

The PDFs of the real cloud/aerosol backscatter, which extends from the noise PDFs, overlaps closely to each other between the daytime and nighttime observations, with the daytime PDF being higher for backscatter>$\sim 10^{-2.5}$ km^{-1} sr^{-1} at most altitudes except for 7.99 km. The day-night differences are less pronounced for smaller backscatter values (e.g., visible and sub-visible cirrus) but increase to 50–100% for larger backscatter values (e.g., convective clouds or cirrus outflows). Studying the PDFs in other

ACPD
10, 17263–17305, 2010

months, we find that the day-night differences may differ somewhat, especially near ~16 km altitudes, but the Januaries of 2007 and 2008 exhibit similar morphology. In an early study with the ICESat data (Dessler et al., 2006), the nighttime cirrus fraction was found to be higher than the daytime, which was mostly due to different detection thresholds used in the daytime and nighttime measurements. Recently, by the same token, Liu and Zipser (2009) analyzed the CALIOP L2 cloud data and reported the similar higher nighttime cloud fraction. As aforementioned, if the $>3\sigma$ threshold were used for CALIOP daytime and nighttime measurements, the nighttime cloud fraction would be higher than the daytime, which is opposite to the day-night differences obtained from the PDF analysis in Fig. 15. The day-night difference is likely dependent on water vapor and temperature, and therefore on cloud ice water content (IWC). As revealed in Fig. 15, if one uses the backscatter as a proxy of IWC, the day-night difference varies with the backscatter value, which can be related to the type of ice clouds and/or to the process controlling cloud formation.

One of the greatest challenges facing with CALIOP cloud/aerosol observations is to measure and compare the features detected in the twilight zones where the measurement noise can change by more than an order of magnitude. The twilight zones in the CALIOP sampling are often in the polar region where some interesting changes have occurred recently in the cloud/aerosol cover. For monitoring/comparing the variations of cloud/aerosol statistics in these regions, separation between the feature and the measurement noise changes become critical and ambiguous with the σ – based approach. Thus, the normalized PDF method may be a promising alternative to provide a quantitative and reliable characterization of cloud/aerosol statistics (e.g., day-night difference, depolarization ratio, and color ratio) in the case where the measurement noise is highly non-stationary and different between two data sets.

ACPD
10, 17263–17305, 2010

5 Conclusions and future work

We developed a research algorithm for cloud/feature detection from a re-gridded CALIOP level 1 backscatter dataset, which will be used for further analyses of the A-Train multi-sensor cloud/aerosol observations. We investigated the noise characteristics and morphologies of the re-gridded CALIOP 532-nm and 1064-nm attenuated backscatters, along with their impacts on cloud/aerosol detection. The modeled molecular scattering was evaluated for all the CALIOP channels using empirically-derived clear-sky profiles. The ratio between empirically-derived and modeled molecular profile is close (<2%) to unity for the nighttime 532-nm TOT data but can vary by 5–10% in the daytime 532-nm TOT data, and by 10–100% in the 1064-nm data. Due to calibration uncertainties with the 1064-nm channel, a fixed scaling ratio (1.2) is applied to the 1064-nm molecular scattering model in the analysis of this study. Although our analyses were focused on measurements in the UT/LS, the methodology and some practical issues apply generally to other atmospheric regions. The major findings and conclusions from this study are summarized as follows.

1. The CALIOP backscatter noises exhibit high-degree spatial variability with the standard deviation (σ) changing by several fold from profile to profile. Such transiency was found in all the three channels, and maps of the noise properties from these channels are presented for January 2008. The daytime noises are significantly higher over landmasses and bright surfaces such snow, ice and desert, reflecting large variability in the received solar background scattering. This large noise variability appears to be more pronounced in the 1064-nm TOT measurements than in the 532-nm backscatter. On the other hand, the nighttime noises, although generally lower than daytime, reveal the patterns associated with strong radiation, such as the South Atlantic Anomaly (SAA) and auroral ovals, in the 532-nm backscatter but not in the 1064-nm data, as expected for dark noise statistics in the type of detector used by these channels.

2. A scaling factor α is used to evaluate CALIOP backscatter calibration by com-

ACPD
10, 17263–17305, 2010

paring the empirically-fitted to modeled clear-sky background. The time series of α reveals some significant changes in the 532-nm and 1064-nm backscatters, which are likely related to different calibration algorithm.

3. Most of the noises in the background-removed CALIOP backscatters behave as a single Gaussian distribution except the nighttime 532-nm PER measurements that have the lowest σ but appear to be associated with two Gaussian-like error sources. These measurement noises are composed of detector/calibration error and natural variability of the solar background scattering.

4. At ~16 km the nighttime PDFs from the 532-nm and 1064-nm TOT backscatters show a drastic change in slope near the value of $\sim 10^{-2.5}$ or $\sim 0.003\,\mathrm{km}^{-1}\,\mathrm{sr}^{-1}$, which is unlikely caused by the attenuation above the cloud layer. This slope transition is difficult to observe with the daytime data due to the large solar noise background. The transition divides the cloud statistics into domains with significantly different properties, which might be useful for studying cirrus generation and lifetime in the TTL (tropical tropopause layer) region. Further investigations with the CALIOP and MLS water vapor and temperature data will provide more insights to this problem.

5. The σ – based detection method in Table 1, which requires a background-removed backscatter, $\Delta\beta(z)$, greater than a multiple σ threshold in two consecutive vertical layers, was developed to detect cloud/aerosol features in the re-gridded CALIOP data. The method was able to produce morphology similar to that from the CALIPSO Level 2 product but showed slightly lower percentages in the Level 2 results. The σ – based detection missed some of the weak signals (e.g., PSCs), which can be detected with a wider horizontal averaging and a lower detection threshold.

6. The observed cloud seasonal variations in the TTL region are consistent among all the CALIOP channels and between this study and the Level 2 results, showing

ACPD
10, 17263–17305, 2010

high cloudiness in December–May and low in July–September. There is no noticeable trend in the daytime σ, but an increasing trend in the nighttime 1064-nm σ is evident, which likely causes the increasing differences between the occurrence frequencies obtained from the 532-nm and 1064-nm channels.

7. The normalized PDFs of the daytime and nighttime backscatters in January 2008 suggest that the cloud occurrence frequency in the TTL region would be higher at 01:30 p.m. than at 01:30 a.m. if a common threshold (e.g., 0.003 km^{-1} sr^{-1}) were applied to both the day and night data. However, this day-night difference is a strong function of the backscatter value, which may be related to the type of ice clouds and/or to the process leading to cloud formation. Small backscatter values (e.g., visible and subvisible cirrus) show a weaker, sometimes reversed day-night difference than the large backscatter values (e.g., convective outflows) in terms of cloud occurrence probability.

By reducing the data volume of the original CALIOP Level 1 data, we are able to process a large quantity of the lidar data and study long-term variability of cloud/aerosol features as well as the measurement noise. With the re-gridded data we are also able to investigate the backscatter and cloud/aerosol properties observed by CALIOP in conjunction with other A-Train observations such as CloudSat and Aura MLS to better understand water content in the upper-tropospheric cirrus and water vapor (e.g., Wu et al., 2010). Because cloud occurrence reduces sharply near the tropopause, accurate and careful statistical analyses are required to extract weak signals in the presence of large and transient noise, This study provides an initial evaluation of CALIOP measurement noise and sensitivity in the tropopause region for the future studies of this kind. With improved understanding and calibration of CALIOP data, we will analyze them jointly with other A-Train data to study potential pollution and aerosol influences on cloud properties in the UT/LS region. As suggested in Jiang et al. (2008), cloud ice particle sizes may vary with polluted and clean environments as pollution aerosols make their way into the UT/LS (Li et al., 2005; Fu et al., 2006; Park et al., 2009).

ACPD
10, 17263–17305, 2010

Acknowledgements. This work was performed at the Jet Propulsion Laboratory, California Institute of Technology, under contract with the National Aeronautics and Space Administration (NASA). We would like to thank Z. Liu, Y. Hu, W. Hunt, C. Trepte, M. Vaughan, and D. Winker for helpful discussions on CALIPSO instrument and data analysis. The data processing by the NASA Langley Research Center Atmospheric Sciences Data Center are gratefully acknowledged.

References

Anselmo, T.: Cloud – Aerosol LIDAR Infrared Pathfinder Satellite Observations: Data Management System, Data Products Catalog. Document No: PC-SCI-503, NASA, Langley Research Center, 2006.

Comstock, J. M., d'Entremont R, DeSlover D., et al.: An intercomparison of microphysical retrieval algorithms for upper-tropospheric ice clouds, B. Am. Meteorol. Soc., 88, 191–204, 2007.

Dessler, A. E., Palm, S. P., Hart, W. D., and Spinhirne, J. D.: Tropopause-level thin cirrus coverage revealed by ICESat/Geoscience Laser Altimeter System, J. Geophys. Res., 111, D08203, doi:10.1029/2005JD006586, 2006.

Dessler, A. E., Zhang, Z., and Yang, P.: Water-vapor climate feedback inferred from climate fluctuations, 2003–2008, Geophys. Res. Lett., 35, L20704, doi:10.1029/2008GL035333, 2008.

Fromm, M. D.: Plumes cover the northern hemisphere: lidar views of summer 2008 volcanic and pyroconvective injections, AGU Fall Meeting, Section A52A, 2008.

Fu, R., Hu, Y., Wright, J. S., Jiang, J. H., Dickinson, R. E., Chen, M., Filipiak, M., Read, W. G., Waters, J. W., and Wu, D. L.: Short circuit of water vapor and polluted air to the global stratosphere by convective transport over the Tibetan Plateau, P. Natl. Acad. Sci., 103, 5664–5669, 2006.

Fu, Q., Hu, Y., and Yang, Q.: Identifying the top of the tropical tropopause layer from vertical mass flux analysis and CALIPSO lidar cloud observations, Geophys. Res. Lett., 34, L14813, doi:10.1029/2007GL030099, 2007.

Hunt, W. H., Winker D. M., Vaughan M. A., et al.: CALIPSO lidar description and performance assessment, J. Atmos. Ocean. Tech., 26(7) 1214–1228, 2009.

Jensen, E. J., Toon, O. B., Selkirk, H. B., Spinhirne, J. D., and Schoeberl, M. R.: On the for-

ACPD

10, 17263–17305, 2010

mation and persistence of subvisible cirrus clouds near the tropical tropopause, J. Geophys. Res., 101, 21361–21375, 1996.
Jensen, E. J. and Ackerman, A. S.: Homogeneous aerosol freezing in the tops of high-altitude tropical cumulonimbus clouds, Geophys. Res. Lett., 33, L08802, doi:10.1029/2005GL024928, 2006.
Jiang, J. H., Su, H., Schoeberl, M., Massie, S. T., Colarco, P., Platnick, S., and Livesey, N.: Clean and polluted clouds: relationships among pollution, ice cloud and precipitation in South America, Geophys. Res. Lett. 35, L14804, doi:10.1029/2008GL034631, 2008.
Li, Q. B., Jiang, J. H., Wu, D. L., et al.: Convective outflow of South Asian pollution: A global CTM simulation compared with EOS MLS observations, Geophys. Res. Lett., 32, 14, L14826, doi:10.1029/2005GL022762, 2005.
Liu, Z.: The CALIPSO lidar cloud and aerosol discrimination: Version 2 algorithm and initial assessment of performance, J. Atmos. Ocean. Tech., 26(7), 1198–1213, 2009.
Liu, Z., Vaughan, M. A., Winker, D. M., Hostetler, C. A., Poole, L. R., Hlavka, D., Hart, W., and McGill, M.: Use of probability distribution functions for discriminating between cloud and aerosol in lidar backscatter data, J. Geophys. Res., 109, D15202, doi:10.1029/2004JD004732, 2004
Liu, Z. Y., Hunt, W., Vaughan, M., et al.: Estimating random errors due to shot noise in backscatter lidar observations, Appl. Optics, 45(18), 4437–4447 2006.
Liu, C. and Zipser, E. J.: Implications of the day versus night differences of water vapor, carbon monoxide, and thin cloud observations near the tropical tropopause, J. Geophys. Res., 114, D09303, doi:10.1029/2008JD011524, 2009.
Lohmann U. and Roeckner, E.: Influence of cirrus cloud radiative forcing on climate and climate sensitivity in a general circulation model, J. Geophys. Res., 100, 16305–16323, 1995.
Mishchenko, M. I., Geogdzhayev, I. V., Rossow, W. B., et al.: Long-Term Satellite Record Reveals Likely Recent Aerosol Trend, Science, 315, p. 1543, 2007.
Park, M., Randel, W. J., Emmons, L. K., and Livesey, N. J.: Transport pathways of carbon monoxide in the Asian summer monsoon diagnosed from Model of Ozone and Related Tracers (MOZART), J. Geophys. Res., 114, D08303, doi:10.1029/2008JD010621, 2009.
Powell, K. A., Hostetler, C. A., Liu, Z. Y., et al.: CALIPSO lidar calibration algorithms: Part I – Nighttime 532 nm parallel channel and 532 nm perpendicular channel, J. Atmos. Ocean. Tech., 26(10), 2015–2033, 2009.
Sassen, K. and Zhu, J.: A global survey of CALIPSO linear depolarization ratios in ice clouds:

ACPD
10, 17263–17305, 2010

Initial findings, J. Geophys. Res., 114, D00H07, doi:10.1029/2009JD012279, 2009.
Sherwood, S. C.: A microphysical connection among biomass burning, cumulus clouds, and stratospheric moisture, Science, 295, 1272–1275, 2002.
Stephens, G. L., Vane, D. G., Tanelli, S., et al.: The CloudSat mission and the EOS constellation: A new dimension of space-based observations of clouds and precipitation, B. Am. Meteorol. Soc., 83, 1771–1790, 2002.
Tanelli, S., Durden, S. L., Im, E., et al.: CloudSat's Cloud Profiling Radar after 1 year in orbit: performance, external calibration, and processing, IEEE T. Geosci. Remote, 48, 3560–3573, 2008.
Thomason, L. W. and Pitts, M. C.: CALIPSO observations of volcanic aerosol in the stratosphere, Proc. of SPIE, 7153, 71530O-7, 2008.
Vaughan, M., Powell, K. A., Kuehn, R. E., et al.: Fully Automated Detection of Cloud and Aerosol Layers in the CALIPSO Lidar Measurements, J. Atmos. Ocean. Tech., 26, 2034–2050, 2009.
Vernier, J. P., Pommereau, J. P., Garnier, A., et al.: Tropical stratospheric aerosol layer from CALIPSO lidar observations, J. Geophys. Res., 114, D00H10, doi:10.1029/2009JD011946, 2009.
Winker, D. M., Pelon, J., and McCormick, M. P.: The CALIPSO mission: Spaceborne lidar for observation of aerosols and clouds, Proc. SPIE Int. Soc. Opt. Eng., 4893, 1–11, 2003.
Winker, D. M., Hunt, W. H., and McGill, M. J.: Initial performance assessment of CALIOP, Geophys. Res. Lett., 34, L19803, doi:10.1029/2007GL030135, 2007.
Winker, D. M., Vaughan, M. A., Omar, A., et al.: Overview of the CALIPSO Mission and CALIOP Data Processing Algorithms, J. Atmos. Ocean. Tech., 26, 2310–2323, 2009.
Wu, D. L., Austin, R. T., Deng, M., et al.: Comparisons of Global Cloud Ice from MLS, CloudSat, and Correlative Data Sets, J. Geophys. Res., CloudSat special section, 114, D00A24, doi:10.1029/2008JD009946, 2009.
Young, S. A. and Vaughan, M. A.: The retrieval of profiles of particulate extinction from Cloud Aerosol Lidar Infrared Pathfinder Satellite Observations (CALIPSO) data: Algorithm description, J. Atmos. Ocean. Tech., 26, 1105–1119, 2009.

ACPD
10, 17263–17305, 2010

Table 1. Cloud/Aerosol detection thresholds used in this study.

	532-nm PER	532-nm TOT	1064-nm TOT
Daytime	Min(5σ, 1×10^{-4})	Min(5σ, 1×10^{-4})	Min(5σ, 1×10^{-3})
Nighttime	Max(80σ, 3×10^{-4})	Max(16σ, 3×10^{-4})	Max(8σ, 3×10^{-4})

ACPD
10, 17263–17305, 2010

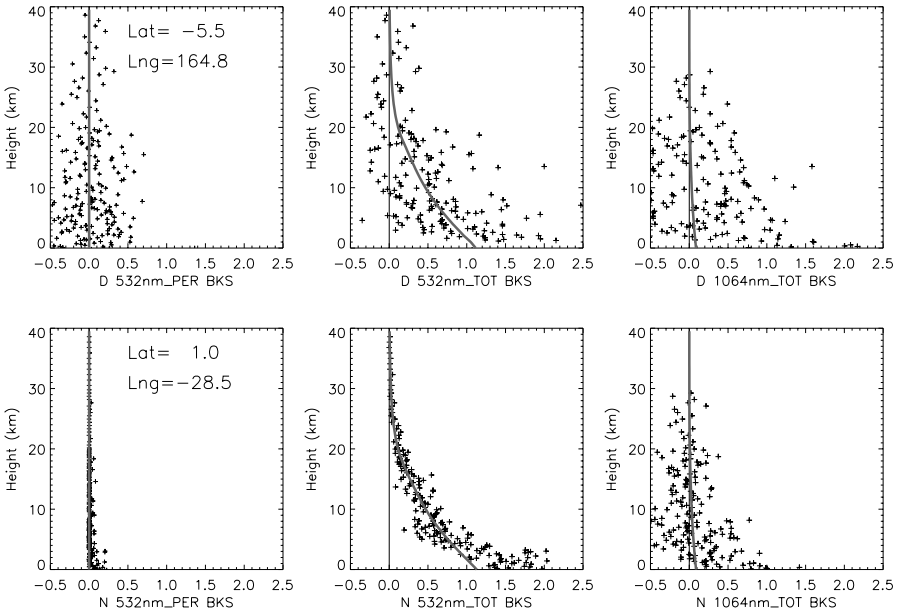

Fig. 1. The attenuated CALIOP backscatter profiles in 10^{-3} km^{-1} sr^{-1} from tropical daytime (top panels) and nighttime (bottom panels) samples on 1 January 2008. The thick grey curve is the background molecular backscatter profile estimated from the atmosphere density (see text). There are no 1064-nm backscatter data at heights above ~30 km. The backscatter is noisier at lower altitudes primarily because of the finer vertical bins (i.e., less integration time per bin).

ACPD
10, 17263–17305, 2010

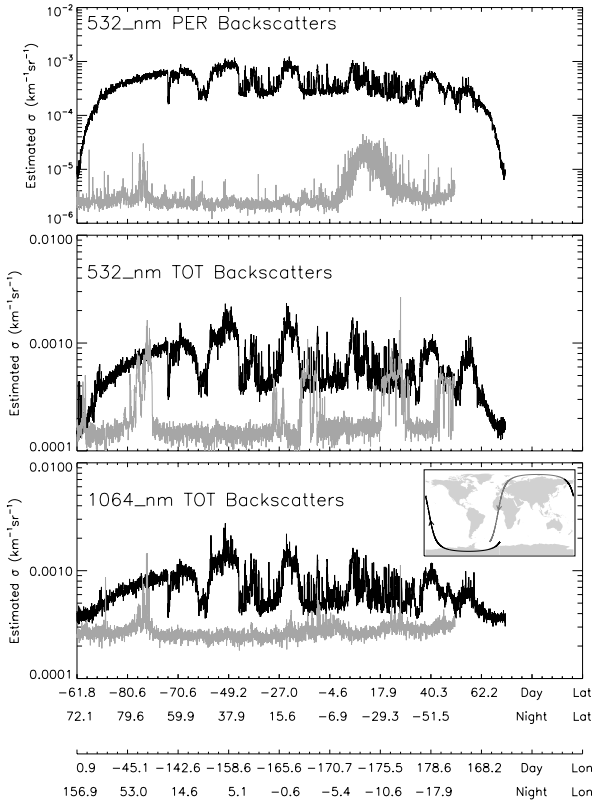

Fig. 2. Orbital variations of the estimated σ of the 532-nm PER (top), 532-nm TOT (middle), and 1064-nm TOT (bottom) backscatter from an orbit (embedded map) on 1 January 2008. The A-Train orbit has a 98° inclination angle and the flight direction is indicated by the arrows in the map. The day (night) portion of the orbit is depicted by black (grey) line. In the night series of 532-nm PER noise, the high σ values to the end of the series are associated with the South Atlantic Anomaly (SAA).

ACPD
10, 17263–17305, 2010

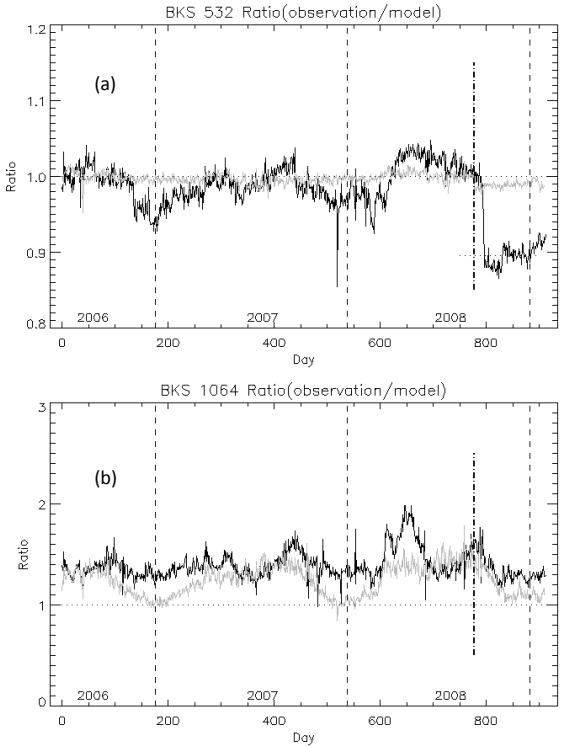

Fig. 3. Time series of the daily averaged scaling factor α, the ratio of empirically-estimated vs. modeled clear-sky background backscatter for daytime (black) and nighttime (grey) data: **(a)** 532-nm TOT and **(b)** 1064-nm TOT. Since individual α values can vary substantially due to measurement noise, individual profiles with a very large value (α>5) are excluded. The year boundary is indicated by the dashed lines, whereas the dash-dotted line indicates the version change from V2.01 to V2.02. There is little variability in the nighttime 532-nm α and the values are close to unity as expected for well-calibrated measurements. The seasonal variation in the nighttime 1064-nm result is likely due to the optically-thin clouds/aerosols that are included in the fitting.

ACPD
10, 17263–17305, 2010

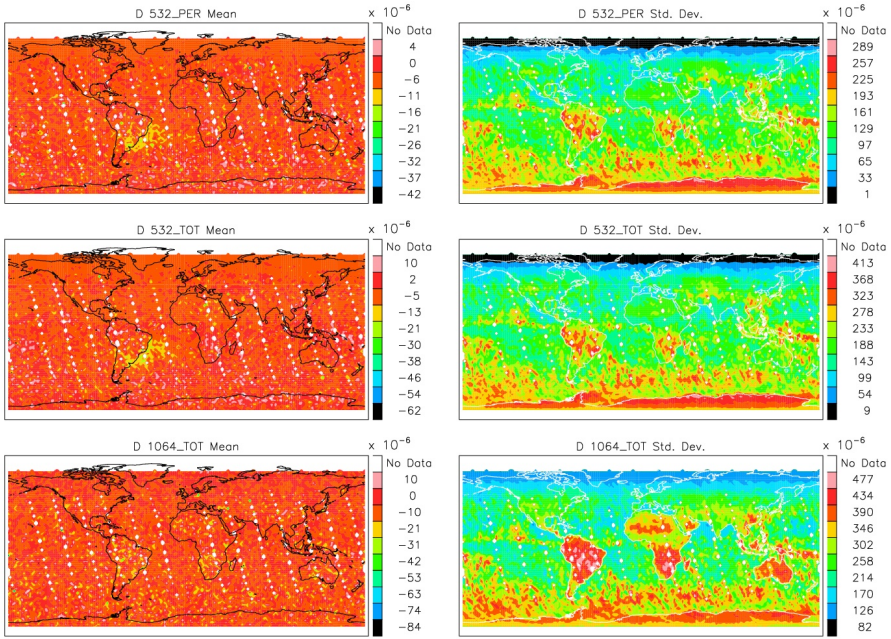

Fig. 4. Monthly mean μ and σ of the daytime 532-nm PER (top), 532-nm TOT (middle), and 1064-nm TOT (bottom) backscatter noise (in $km^{-1}\ sr^{-1}$) for January 2008. The 2°×2° longitude-latitude grid is used for averaging. The majority portion of the daytime orbits is ascending (i.e., latitude increasing with time). The descending portion of the orbits is excluded to minimize the mixed statistics between the two local times.

ACPD
10, 17263–17305, 2010

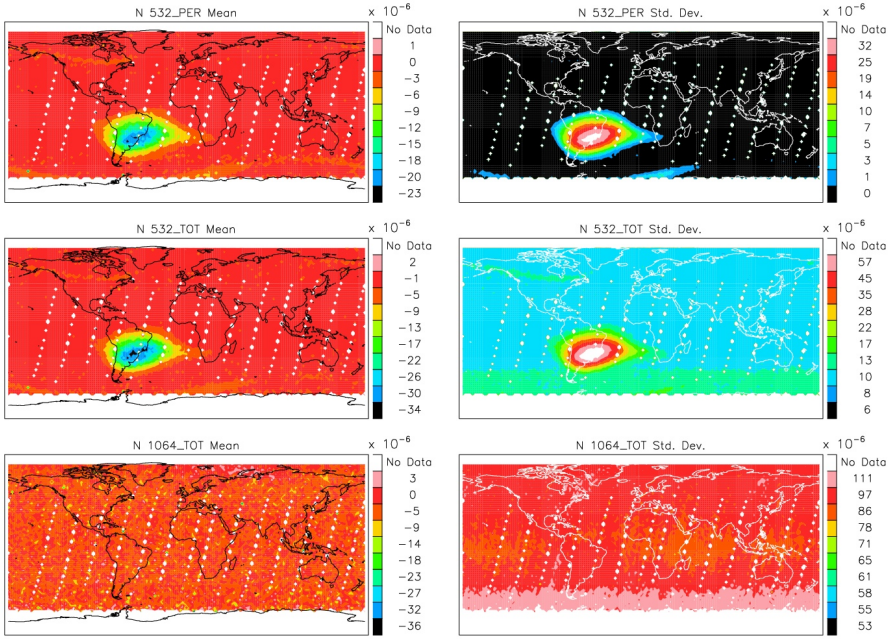

Fig. 5. As in Fig. 4 but for the nighttime backscatter noise, and the ascending portion of the orbits are excluded in these maps.

ACPD
10, 17263–17305, 2010

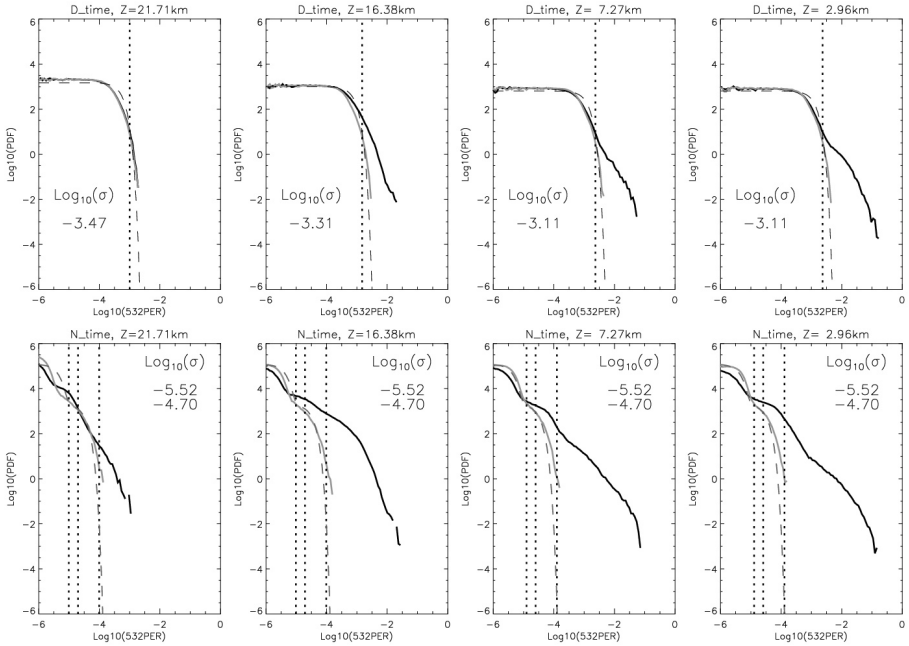

Fig. 6. Normalized PDFs of the daytime (upper panels) and nighttime (lower panels) 532-nm PER backscatter from a tropical (10° S–10° N) bin for January 2008. The estimated σ is shown in each panel and the vertical dotted lines indicate the 3σ value for daytime, and 1σ, 2σ, and 10σ for nighttime. The grey curve is the PDF of negative values folded onto the positive side and the dashed line is the analytical Gaussian function for the estimated σ. The PDFs are plotted in a log-log scale with backscatter in km^{-1} sr^{-1} and PDF in km sr. The PDF is normalized such that its integration over all backscatter bins is equal to unity. The sharp rising PDF at backscatter $<3\sigma$ indicates the measurement noise distribution (e.g., Gaussian). A double-Gaussian noise characteristic is evident in the nighttime PDFs, where the dashed line represents an analytical double-Gaussian function for the standard deviations listed and partitioned with 90% and 10% respectively. The SAA contribution is excluded in the statistics at this latitude bin.

ACPD
10, 17263–17305, 2010

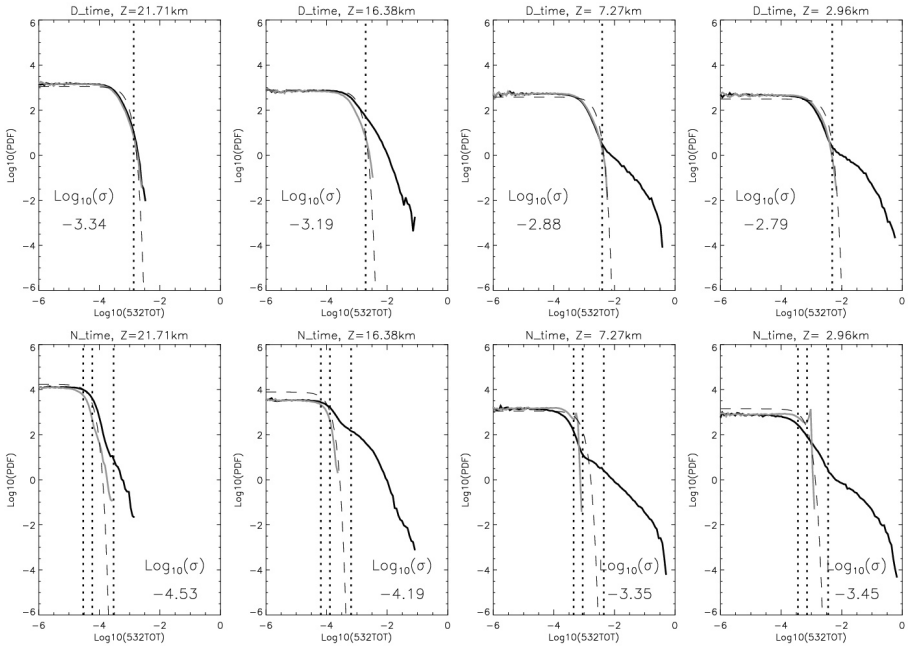

Fig. 7. As in Fig. 6 but for the 532-nm TOT backscatter. The spike and sharp cutoff in the nighttime PDF of negative backscatter values is a manifestation of strong cloud/aerosol attenuation. It is less obvious in the daytime data that are noisier. At 7.27 and 2.96 km, the σ value is somewhat overestimated and the noise PDF deviates slightly from the Gaussian due to the non-stationary characteristics of CALIOP measurement noise.

ACPD
10, 17263–17305, 2010

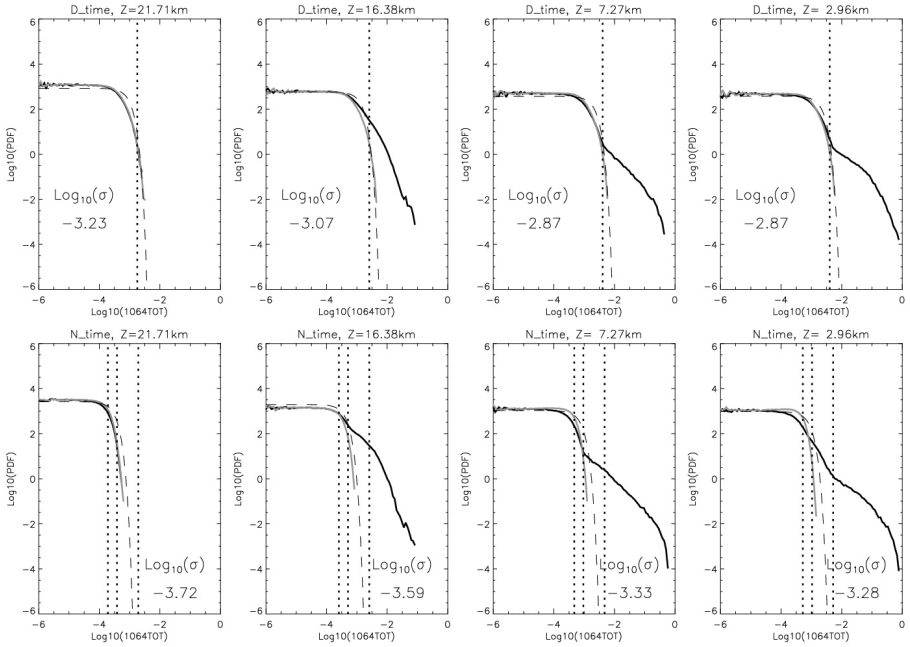

Fig. 8. As in Fig. 6 but for the 1064-nm TOT backscatter.

ACPD
10, 17263–17305, 2010

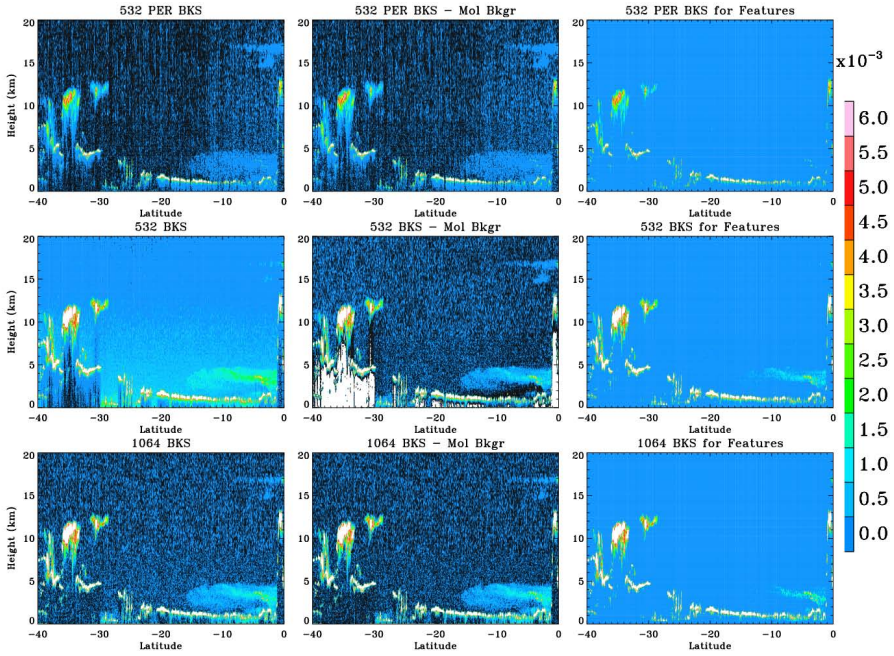

Fig. 9. The 532 and 1064 attenuated TOT backscatters, the backscatters greater than the modeled molecular backscatter, and the features detected using the thresholds in Table 1 for the nighttime orbit in Fig. 2. The thresholds in Table 1 are relatively conservative and select most of the cloud features but miss some of the aerosol and cirrus features between 15° S and the equator.

ACPD
10, 17263–17305, 2010

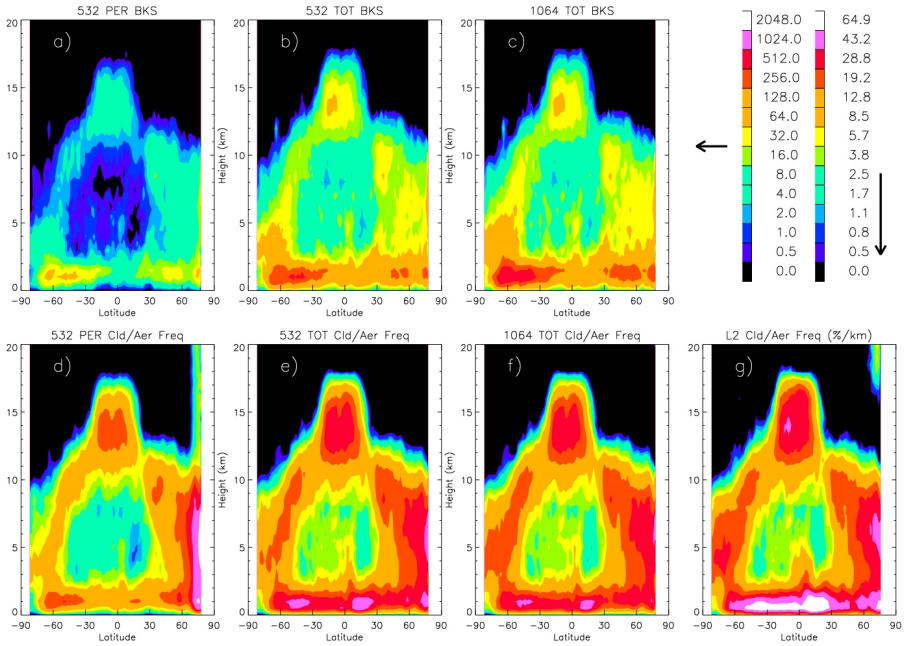

Fig. 10. Daytime zonal mean backscatter and cloud/aerosol occurrence frequency for January 2008: **(a–c)**, respectively, the zonal mean 532-nm PER, 532-nm TOT, and 1064-nm TOT attenuated backscatter in $km^{-1}\,sr^{-1}$; **(d–f)** the corresponding occurrence frequencies by altitude (in %/km) for cloud/aerosol features detected from these channels; and **(g)** the total occurrence frequency of clouds and aerosols from the L2_Clay and L2_Alay data. The overlapping portions in the L2 data are removed in compiling these statistics.

ACPD
10, 17263–17305, 2010

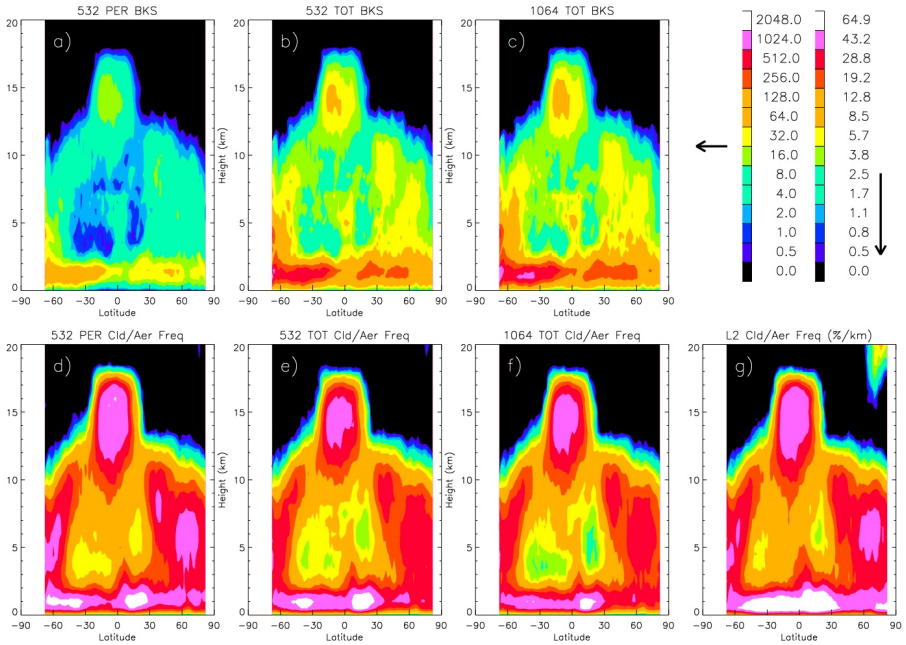

Fig. 11. As in Fig. 10 but for the nighttime data. In the nighttime 532-nm PER statistics, despite the aggressive screening threshold (80σ), a fraction (~0.5%) of stratospheric features (not PSCs) are still present at middle latitudes, which warrants further investigation.

ACPD
10, 17263–17305, 2010

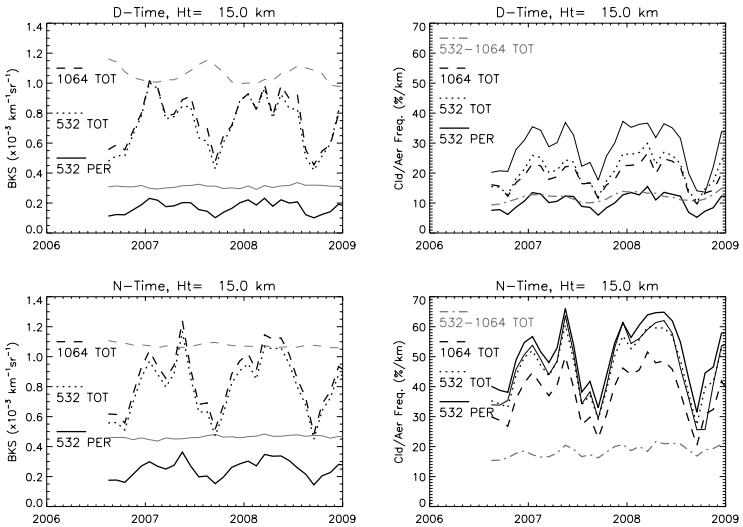

Fig. 12. Time series of daytime (top panels) and nighttime (bottom panels) monthly mean backscatter (left) and cloud occurrence frequency (right) at 15 km altitude in the 10° S–10° N latitude bin. The 532-nm and 1064-nm TOT are the feature backscatters, in which the molecular scattering contributions have been subtracted out. The 532-nm depolarization ratio ($\delta = \beta_{\perp}/\Delta\beta_{//}$) and the 1064/532 color ratio are calculated from these monthly means and plotted, respectively as the thin grey solid and dashed lines in the left panels. In the occurrence frequency time series (right panels), the L2 05km (CLay+ALay) data (thin grey line) is also included to compare with the results from this study. The occurrence frequency of multi-layer features is a function of height in all the frequency cases, representing the probability of feature occurrence per unit height bin. A decreasing trend in the color ratio is evident in both daytime and nighttime data. An increasing difference between the occurrence frequencies at 532 and 1064 nm is evident, especially in the nighttime data, which is likely due to the dark count increases in the 1064 nm channel (see text).

ACPD
10, 17263–17305, 2010

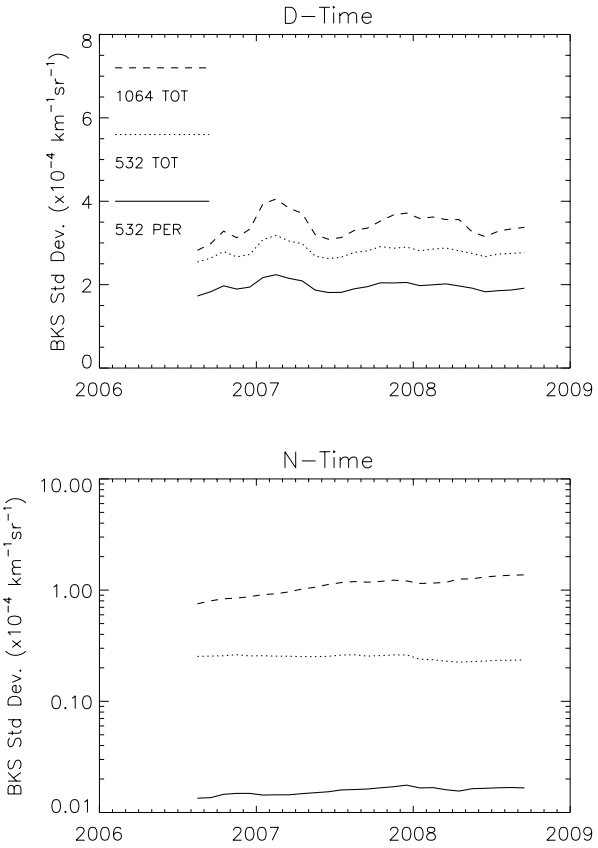

Fig. 13. Time series of daytime (top) and nighttime (bottom) mean single-profile standard deviations of the 532-nm PER, 532-nm TOT and 1064-nm TOT backscatter in the 10° S–10° N bin. The increasing trend in the 1064-nm channel is consistent with the dark count increase reported by Hunt et al. (2009).

ACPD
10, 17263–17305, 2010

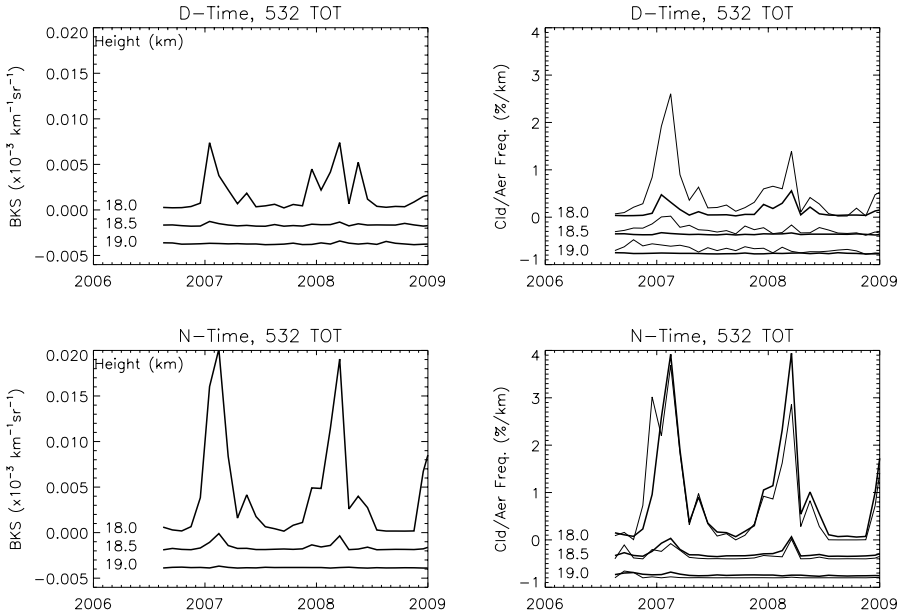

Fig. 14. Seasonal variations of the features detected from the 532-nm TOT backscatter near the tropical (10° S–10° N) tropopause where the sharp transition with height occurs. For the monthly backscatter time series (left panels), the values at altitudes above 18 km are offset by an increment of 0.002 km^{-1} sr^{-1}, whereas for the occurrence frequency (right panels) they are offset by 0.4%/km. The monthly cloud/aerosol occurrence frequencies from this study and from the L2 5km (CLay+ALay) data are respectively denoted by thick and thin lines. The daytime (nighttime) 19 km mean values of occurrence frequency are 0.036 (0.059)%/km from this study and 0.13 (0.011)%/km from the L2 data.

ACPD
10, 17263–17305, 2010

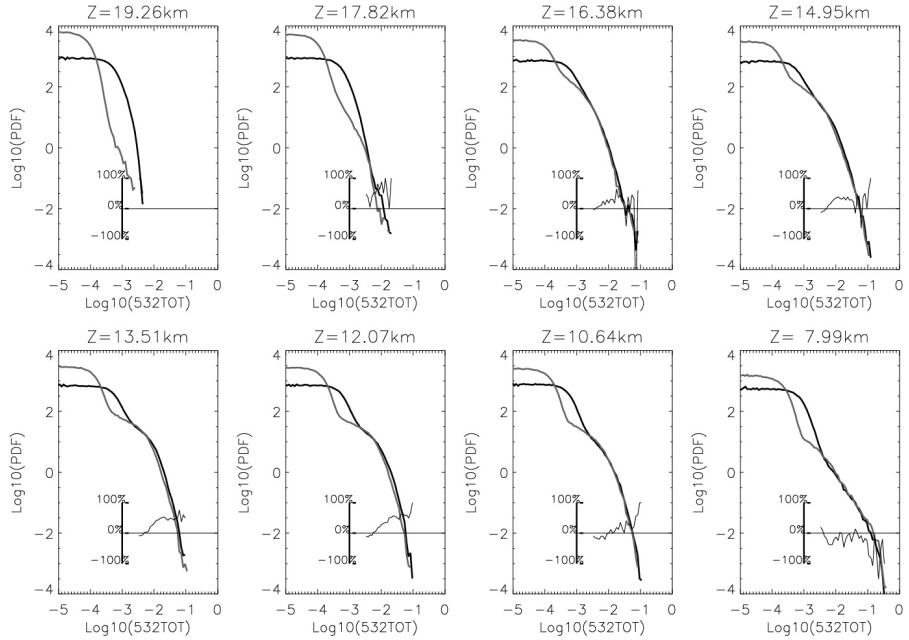

Fig. 15. Day-night differences of the normalized PDFs for the 532-nm TOT backscatter in the upper tropospheric tropics (10° S–10° N) for January 2008. Daytime and nighttime PDFs are shown in dark and grey line, respectively, whereas the thin line beneath PDF curves is the percentage PDF difference, which is value-dependent. The rising PDF at small values is a manifestation of the noise distribution, showing higher daytime noise at all levels. The PDF differences in the daytime-noise area and at smaller values are not shown. The daytime PDFs are generally higher than the nighttime at most altitudes except at 7.99 km. The day-night difference, in terms of probability density of cirrus occurrence, increases at backscatter values between $10^{-2.5}$ and $\sim 10^{-2}$ km^{-1} sr^{-1}, but remains approximately constant for the values $>\sim 10^{-2}$ km^{-1} sr^{-1}, at altitudes >12 km. Analyses from other months show similar PDF characteristics in the day-night differences.

ACPD
10, 17263–17305, 2010